doi:10.1016/j.jmb.2012.05.039 J. Mol. Biol. (2012) 422, 414–428

Contents lists available at www.sciencedirect.com

Journal of Molecular Biology

journal homepage: http://ees.elsevier.com.jmb

Maximizing Detergent Stability and Functional Expression of a GPCR by Exhaustive Recombination and Evolution

Karola M. Schlinkmann [1], Matthias Hillenbrand [1], Alexander Rittner [1], Madeleine Künz [1], Ralf Strohner [2] and Andreas Plückthun [1]*

[1]*Department of Biochemistry, University of Zurich, Winterthurerstrasse 190, 8057 Zurich, Switzerland*
[2]*Sloning Group at MorphoSys AG, Lena-Christ-Strasse 48, 82152 Martinsried/Planegg, Germany*

Received 23 March 2012;
received in revised form
27 May 2012;
accepted 30 May 2012
Available online
6 June 2012

Edited by J. Bowie

Keywords:
in vitro DNA recombination;
screening and selection;
plasmid copy number;
membrane protein
expression;
coevolution

To identify structural features in a G-protein-coupled receptor (GPCR) crucial for biosynthesis, stability in the membrane and stability in detergent micelles, we developed an evolutionary approach using expression in the inner membrane of *Escherichia coli*. From the analysis of 800,000 sequences of the rat neurotensin receptor 1, in which every amino acid had been varied to all 64 codons, we uncovered several "shift" positions, where the selected population focuses on a residue different from wild type. Here, we employed *in vitro* DNA recombination and a comprehensive synthetic binary library made by the Slonomics® technology, allowing us to uncover additive and synergistic effects in the structure that maximize both detergent stability and functional expression. We identified variants with >25,000 functional molecules per *E. coli* cell, a 50-fold increase over wild type, and observed strong coevolution of detergent stability. We arrived at receptor variants highly stable in short-chain detergents, much more so than those found by alanine scanning on the same receptor. These evolved GPCRs continue to be able to signal through the G-protein. We discuss the structural reasons for these improvements achieved through directed evolution.

Introduction

G-protein-coupled receptors (GPCRs) constitute the largest group of cell-surface receptors found in nature. GPCRs are involved in all kinds of signaling processes, giving this class of proteins enormous pharmacological relevance. Currently, it is estimated that 30% of all marketed drugs target GPCRs.[1,2] However, our understanding of GPCR architecture and mechanism has remained limited, and the design features of agonists and antagonists for the diverse set of receptors have remained mostly enigmatic. Low expression levels, poor biophysical behavior of solubilized GPCRs and their intrinsic conformational flexibility make their structural characterization very challenging. For the same reasons, drug screening remains largely limited to assays in whole cells.

The first crystal structure of a GPCR, bovine rhodopsin, was solved in the year 2000 and remained unchallenged for several years. Recently, GPCR structures of the inactive states of the human adenosine receptor A_{2A},[3] human β2-adrenergic

*Corresponding author. E-mail address: plueckthun@bioc.uzh.ch.

Present address: M. Künz, Institute for Biochemistry and Molecular Biology, Laboratory for Structural Biology of Infection and Inflammation, University of Hamburg, c/o DESY Bldg. 22a, Notkestrasse 85, 22607 Hamburg, Germany.

Abbreviations used: GPCR, G-protein-coupled receptor; StEP, staggered extension process; MFI, mean fluorescence intensity; DDM, *n*-dodecyl-β-D-maltopyranoside; CHS, cholesteryl hemisuccinate; DM, *n*-decyl-β-D-maltopyranoside; NM, *n*-nonyl-β-D-maltopyranoside; OG, *n*-octyl-β-D-glucopyranoside; HTG, *n*-heptyl-β-D-thioglucopyranoside; RLBA, radioligand binding assay; EDTA, ethylenediaminetetraacetic acid.

receptor,[4,5] turkey β1-adrenergic receptor,[6] C-X-C chemokine receptor type 4[7] and human dopamine D3 receptor[8] were determined. In most cases, crystallization was enabled by allowing efficient crystal contact formation by fusion protein strategies (e.g., Ref. 4); however, this strategy hampers functional characterization, as it prevents binding of the G-proteins. In some cases, receptor stability was also improved by mutagenesis.[6,9] First insight into the signaling process itself was provided by the determination of the structure of the complex of the β2-adrenergic receptor with the heterotrimeric G-protein.[10]

In our laboratory, we had previously developed a FACS (*f*luorescence-*a*ctivated *c*ell *s*orting)-based selection system to evolve and engineer further GPCRs for high functional expression and stability in detergents and have successfully applied it to several GPCRs.[11,12] More importantly, we wished to exploit this technology to elucidate and understand the structural features that determine biosynthesis, stability in the bilayer membrane and, after solubilization, stability in detergent micelles. This will help describe the evolutionary forces that have shaped this family.

Because of the incomplete coverage of mutant space by random mutagenesis, we recently performed an exhaustive saturation mutagenesis to determine, for every position of rNTR1-D03, the amino acid residues that are not permitted, are permitted and are preferred.[13] The already improved mutant rNTR1-D03 was used as framework,[11] since rNTR1-wt expression levels were so low that they would not allow these experiments. Here, we have generated both shuffled and exhaustive designed synthetic DNA libraries for selection of the optimal combination of shift mutations with respect to expression levels and stability in detergents. Receptor variants with unanticipated gains in functional expression and stability in detergents were generated, which maintained the ability to signal through G-proteins, allowing us to now formulate detailed structural hypotheses of the architectural basis of such biophysical improvements.

Results

Library design

In a previous comprehensive randomization study, every receptor position had been turned into a separate NNN library representing all 64 codons.[13] Thus, 376 position-specific libraries were created and then selected for high functional expression using our previously developed FACS-based approach.[11] The selected library pools were analyzed by deep sequencing, and the evaluation of 800,000 sequences led to the identification of 30 shift positions (Table 1, see M30), defined as those

Table 1. Sequence of NTR1-related evolved GPCRs at crucial positions

	TM1							TM2							TM3			I2		TM4		E2		TM5			TM6			E3		TM7	
D03 reference	V	N	T	I	F	S	A	T	A	D	L	M	E	L	R	D	C	A	A	I	M	K	V	I	I	N	K	C	Y	C	F	T	F
NTR1 position (aa)	57	58	68	70	75	83	86	101	110	113	119	121	124	125	143	150	172	177	201	202	208	235	240	253	260	262	263	320	324	332	342	354	358
Ballesteros–Weinstein			1.36	1.38	1.43	1.51	1.54	2.38	2.47	2.50	2.56	2.58	2.61	2.62	3.26	3.33	3.55		4.57	4.58	4.64	5.36	5.41	5.54	5.61	5.63	5.64	6.47	6.51	6.59		7.38	7.42
M30	I	R	S	L	L	G		R	L	S	F	L	D	V	K	E	R	H	S	L	V	R	L	A		R	R	L	L	V		S	V
M303	I	R	S	L	L	G	L	R	L	S	F	L	D	V	K	E	R	H	S	L	V	R	L	A	A	R	R	L	L	V	A	S	V
C7E02	I	R	S	L	L	G	L								K	E								A							A	S	V
L5X	I				L			R		S	F	L			K	E		H					L	A			L		V		S	V
TM86V							L																	A									V

positions where selection has focused on a new residue that is different from rNTR-D03 (abbreviated as D03).[13] Each single shift mutation positively affects expression levels, and some of these also significantly increase receptor stability in detergent. Shifts often come in clusters, where shifted residues close in space appear to address the same structural problem independently.[13] Hence, from simply combining the mutations, additivity does not necessarily result, and the optimal combination of shifted residues cannot be deduced directly. We thus explored the combinatorial space of the shift mutations experimentally. Here, we used two independent approaches to create such libraries, and we selected them for variants of highest expression and stability in detergent to bring out the crucial structural features more clearly than would be possible with a single mutation set.

In a first approach, we created a library by *in vitro* DNA shuffling of two genes, (i) D03 (having no shift mutations) with (ii) a synthetic gene carrying all shift mutations at once (termed M30) (Table 1). Methods based on shuffling are straightforward to carry out[14,15] but are not comprehensive in the combinations they generate, since the number of crossovers per gene is limited; thus, the chance of separating two mutations very closely spaced in sequence is finite.

In a second approach, a true "binary" library was synthetically constructed with codons of both D03 and shift amino acids in question at equal frequency at each shift position. This very comprehensive approach requires a demanding synthesis, for which the Slonomics® technology is one of the very few technologies available.[16,17] Both libraries were selected using our established FACS technique,[11] and the selection output was screened for detergent-stable variants.

In a third approach, guided by the statistics of occurrence of particular shift mutations and their biophysical properties when known, we combined several of these mutations to rationally engineer a detergent-stable variant directly.

In vitro DNA shuffling of D03 and M30 by the staggered extension process

We created a diverse DNA library (StEPM30) by *in vitro* DNA shuffling of the D03 with the M30 gene by means of the staggered extension process (StEP)[14,15] (see Supplementary Fig. S1 for illustration). Briefly, an equimolar mixture of D03 and M30 genes was used as input for PCR, in which extremely short elongation cycles (6 s) allow for only short primer extensions. By this staggered extension, the elongated primer fragment can switch templates after the subsequent denaturation step, and 125 cycles are performed to eventually obtain a chimeric full-length PCR product. While carrying out these studies, Shibata *et al.*reported the identification of NTS1-7m,[18] an rNTR1 mutant that is somewhat more stable than rNTR1-wt. NTS1-7m contains four point mutations, A86L$^{1.54}$, I260A$^{5.61}$, F342A (loop E3) and F358A$^{7.42}$. We use the sequential numbering in plain text and the Ballesteros–Weinstein numbering[19] as superscript: here, the first number denotes the helix in sequential order; the second number defines the position within the helix, where the most conserved position of a helix is denoted as x.50, counting downwards toward the N-terminus and upwards to the C-terminus. We had previously identified the strong shift mutation F358V$^{7.42}$ in the D03 background, and thus, we decided to include the mutations A86L$^{1.54}$, I260A$^{5.61}$ and F342A in a further StEP library (termed StEPM303).

The theoretical library diversities of 2^{30} ($\approx 1\times10^9$) for the StEPM30 library and 2^{33} ($\approx 8\times10^9$) for the StEPM303 library cannot be reached in practice due to limited recombination of mutations close in sequence in the StEP method, even though libraries with this number of colonies can easily be created in our *Escherichia coli*-based system. Here, after optimization of StEP parameters such as $MgSO_4$ and primer concentration as well as extension time, recombination events as short as within a 30-bp distance were obtained.

Selection of the StEP library for high functional expression

The initial libraries were subjected to three rounds of StEP shuffling, each followed by three to six rounds of selection by FACS,[11] before expression reached a stable plateau. StEPM30 and StEPM303 selections were pooled for a final selection round, testing both expression at 20 °C and 30 °C (C6_20 and C6_30; Fig. 1a). The mean fluorescence intensity (MFI) of the selected libraries, a measure of the mean functional expression, reached 2-fold of D03 (Fig. 1a). Single-clone expression levels were increased 2.5- to 3-fold, compared to D03 (Fig. 1b) (a 30-fold increase compared to rNTR1-wt), and the best variants reached 12,000 receptors per cell. Sequencing of 87 selected individual variants verified that both favorable and unfavorable shifts are efficiently selected for and against, respectively (Fig. 1c).

C332V$^{6.59}$ is the most dominant shift after selection for functional expression, occurring in >90% of selected variants. Shifts further accumulate in TM5, with a focus on I253A$^{5.54}$. TM5 is involved in conformational changes of the receptor upon activation, and its conformational flexibility might provide ample opportunity for improvements. Not all shift mutations originally selected as single shift mutations were maintained in the context of other shift mutations, such as C320L$^{6.47}$ and Y324L$^{6.51}$ (<20% frequency), which are close in sequence to the dominant shift C332V$^{6.59}$ (Fig. 1c). Because of the

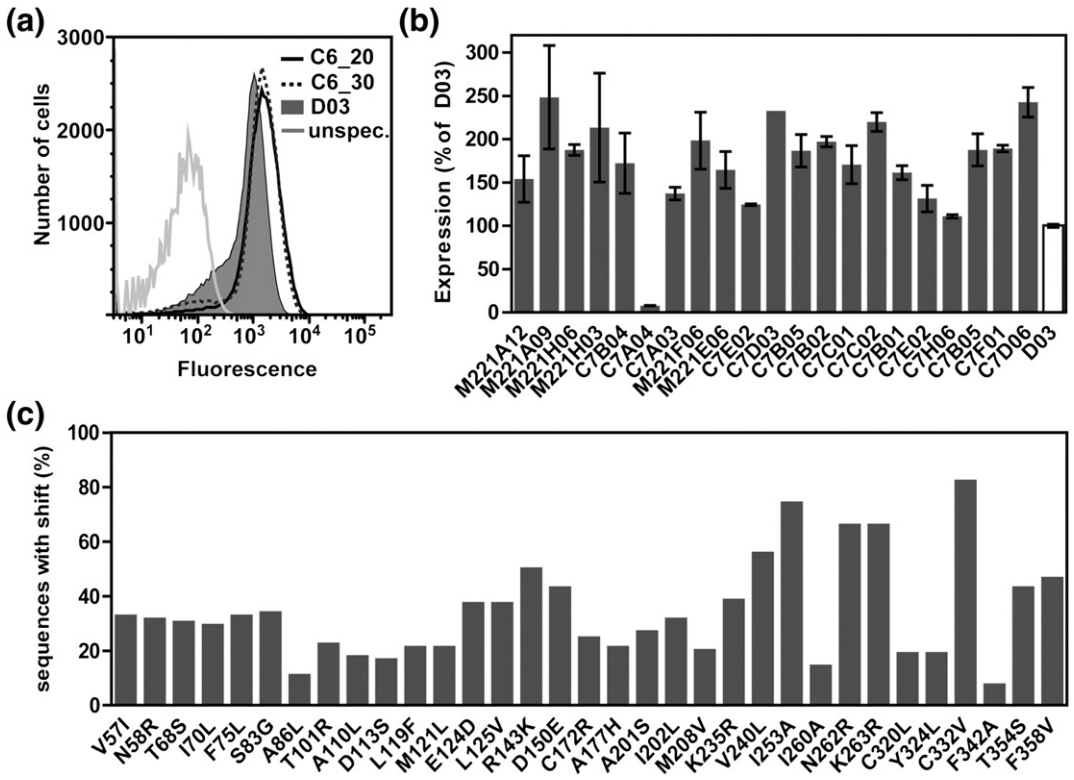

Fig. 1. StEP selections. (a) Expression profiles of final StEP selection pools after 20 h expression at 20 °C (C6_20) and 30 °C (C6_30). Expression is measured as binding of BODIPY-NT(8–13) to receptors and analyzed by flow cytometry. The MFIs of C6_20 and C6_30 are 1660 and 1550, compared to 880 for D03. Nonspecific binding of BP-NT(8–13) is measured in the presence of excess unlabeled neurotensin (10 μM). (b) Expression levels of individual selected StEP variants. Receptors per cell were quantified by RLBA with 15 nM [^{3}H]neurotensin. An average of two independent experiments is given. (c) Frequency of sequences carrying the shift mutation in the final StEP selection pools (C6_20 and C6_30). We sequenced and analyzed 87 individual variants.

incomplete crossover, some shifts might be selected together, displaying a neutral phenotype in the context of other functionally relevant shifts. Interestingly, the shift mutations A86L$^{1.56}$, I260A$^{5.61}$ and F342A (E3 loop), originating from the StEPM303 library and introduced from NTS1-7m, are underrepresented after selection and, thus, must be disfavored in the context of the other selected shift mutations. Thus, it appears that an alternative, more robust solution has been found by our combinatorial approach (see below).

Detergent stability of receptor variants evolved by StEP

Next, we analyzed the stability of selected variants in different detergents, essentially as described previously.[12] About 90% of the selected variants are more stable than D03 in a mild detergent mixture of *n*-dodecyl-β-D-maltopyranoside (DDM), 3-[(3-cholamidopropyl)dimethylammonio]-1-propanesulfonate (Chaps) and cholesteryl hemisuccinate (CHS), supplemented with 30% glycerol, and the most stable variants retain full activity after 20 min at 45 °C (Fig. 2a). The apparent T_m of the variants M221H03 and M221A09 is 65 °C, an increase of 25° compared to D03 (Fig. 2b). The heat-induced inactivation of the receptors is irreversible, and T_m thus reflects the transition point of heat-induced deactivation after a defined incubation. The dramatic increase in detergent stability was intriguing, considering that this particular property was never under direct selection pressure, hence suggesting a strong correlation between functional expression and detergent stability.

Since glycerol is unfavorable for crystallization, we attempted to identify variants that are stable in its absence. In the absence of glycerol, CHS and Chaps, i.e., with DDM as the sole detergent (buffer SABoDDM), we observed a stronger separation of stable from unstable clones, with the most stable variant being C7E02 (Fig. 3a, C7E02 highlighted in black). The apparent T_m of C7E02 under these conditions is 52 °C, a 20° increase compared to D03 (31 °C; Table 2 and Supplementary Fig. S2a). Moreover, C7E02 retains about 75% activity after 24 h at 4 °C, while D03 looses activity during that time (Supplementary Fig. S2b).

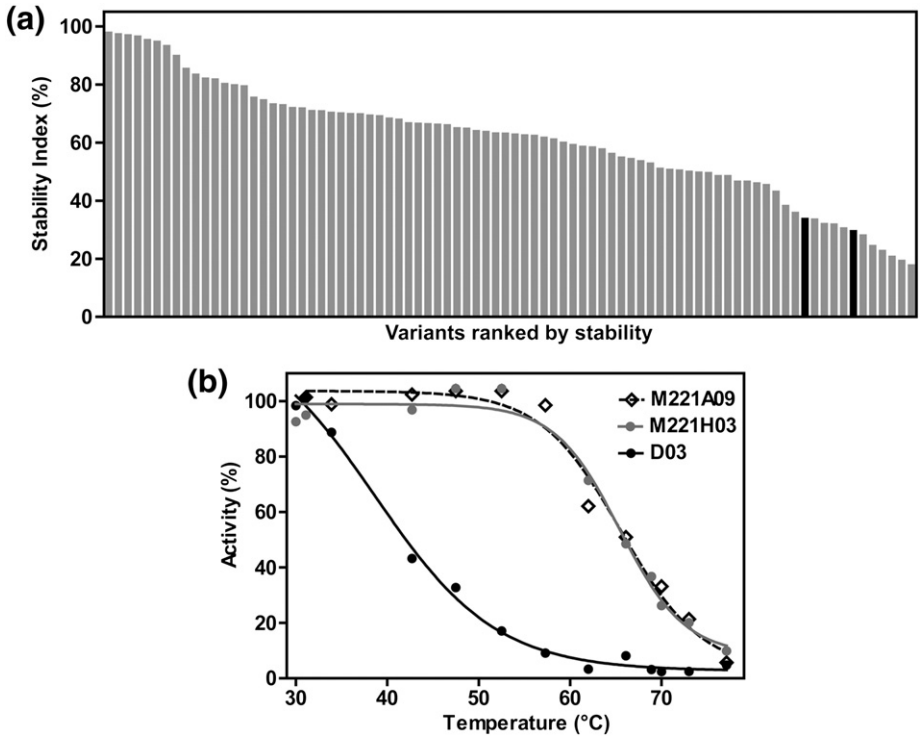

Fig. 2. Stability screening of evolved StEP variants in buffer SAB, ranked by stability. (a) Stability screening in buffer SAB (0.1% DDM, 0.5% Chaps, 0.1% CHS and 30% glycerol). The stability index is the ratio of remaining ligand binding activity after 20 min of incubation at 45 °C compared to incubation at 4 °C. Screening was performed in the ligand-free state. Black bars represent two independent measurements for D03. (b) Thermal denaturation profiles of the most stable evolved StEP variants in buffer SAB. Thermal denaturation was measured in the ligand-free state after 20 min at the indicated temperature. D03 displays an apparent T_m of 39 °C, compared to 65 °C for M221H03 and M221A09. Data from a representative measurement are shown.

In the larger micelles that are formed by longer-chain detergents, the protein part is prevented from making crystal contacts, making the mild detergent DDM unfavorable for membrane proteins devoid of large extracellular regions.[20] We have thus rescreened our best variants in shorter and harsher detergents (Fig. 3b, C7E02 highlighted in black). D03 is essentially unstable in *n*-decyl-β-D-maltopyranoside (DM; buffer SABoDM) with an apparent T_m of approximately 18 °C, while C7E02 quantitatively retains protein activity with an apparent T_m of 41 °C (Table 2 and Supplementary Fig. S2c). All other variants were completely inactivated upon buffer exchange to DM, and detergents shorter than DM

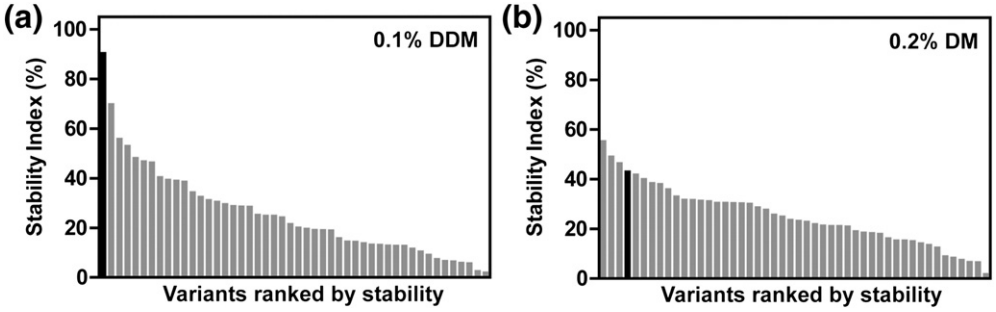

Fig. 3. Stability screening of evolved StEP variants in buffers SABoDDM and SABoDM, ranked by stability. (a) Stability screening in buffer SABoDDM (0.1% DDM as the sole detergent) and (b) buffer SABoDM (0.2% DM as the sole detergent). C7E02 is highlighted in black bars; D03 is inactive in (a) and (b). The stability index is the ratio of remaining ligand binding activity after 20 min of incubation at 45 °C compared to incubation at 4 °C. Screening was performed in the ligand-free state.

Table 2. Melting temperatures (°C) of evolved GPCRs in detergents

	DDM		DM		NM	OG
	+NT	−NT	+NT	−NT	+NT	+NT
rNTR1-wt	40	29	34	(17)	36	(15)
D03	47	31	42	(18)	35	(14)
C7E02	56	52	51	41	45	30
TM86V	59	46	53	37	48	38
L5X	58	42	53	33	50	40
NTS1-7m[a]	50	37	45	27	39	27
wt-TTM	48	41	43	27	38	26

$n = 2–9$; average error ± 2 °C.

Numbers in parentheses are approximate values, since the protein is too unstable.

[a] Reconstructed according to Ref. 18.

also lead to complete inactivation of C7E02. Reaching stability in such detergents thus required further engineering (see below).

Conformational stabilization of GPCRs by agonist or antagonist binding proved to be a prerequisite for all GPCR structures solved so far (except opsin[21]). Here, we assessed the influence of agonist binding on detergent stability. Agonist stabilization of C7E02 allowed detergent exchange to *n*-nonyl-β-D-maltopyranoside (NM) and *n*-octyl-β-D-glucopyranoside (OG) (Table 2 and Supplementary Fig. S3). The apparent T_m of C7E02 in OG is 30 °C (Table 2 and Supplementary Fig. S3d), a condition under which D03 and rNTR1-wt are essentially unstable (estimated T_m of 14–15 °C; Table 2 and Supplementary Fig. S3d).

C7E02 combines 14 mutations in addition to those present in D03 (Table 1), 13 of which are shift mutations, plus an unrelated mutation R183L$^{4.39}$ located at the cytoplasmic end of TM4, which was most likely introduced during the numerous StEP-PCR cycles (Supplementary Fig. S1). As a single shift, R183L$^{4.39}$ did not significantly influence detergent stability (data not shown). Interestingly, C7E02 does not contain the dominant shift C332V$^{6.59}$. In summary, the evolutionary approach has yielded a clone that is stable in the short-chain detergent OG in the presence of agonist, which is a dramatic improvement, as our previously evolved molecule D03 is essentially unstable in OG.

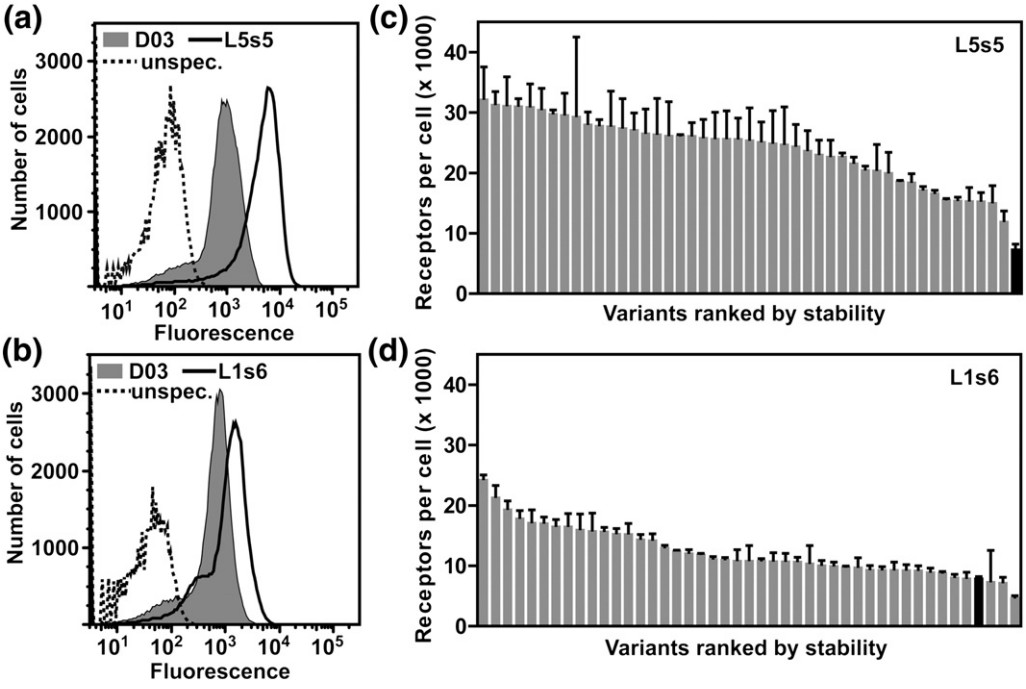

Fig. 4. Slonomics® library selections. (a and b) Expression profiles of final L5 (a) and L1 (b) selections compared to D03. Results for expression at 30 °C are shown. Expression is measured as binding of BODIPY-NT(8–13) to receptors and analyzed by flow cytometry. Nonspecific binding of BOPIPY-NT(8–13) is measured in the presence of excess unlabeled neurotensin (10 μM). (a) After five rounds of selection for high functional expression by FACS, the final evolved L5s5 pool (MFI, 5200) shows a 5-fold increase in MFI compared to D03 (MFI, 970). (b) The final evolved L1s6 pool shows a MFI of 1300 after six selection rounds, a 2-fold increase in MFI compared to D03 with MFI of 670. (c and d) Expression levels of individual selected L5s5 (c) and L1s6 (d) variants (30 °C, 20 h). Receptors were quantified by RLBA with 15 nM [^{3}H] neurotensin. Duplicates of a representative experiment are given. Black bars give the expression level of the respective D03 control.

Comprehensive binary combinatorial library made by Slonomics® technology

Given the success of the StEP libraries but the limitation of having an incomplete separation of mutations closely spaced in sequence, we aimed to generate a comprehensive "binary" library, covering all theoretically possible residue combinations of D03 or M303. The library was synthesized *de novo* using the modified Slonomics® technology for DNA library synthesis.[16,17] Most importantly, to exclude any effects of the nucleotide sequence on the outcome due to codon usage, tRNA levels or mRNA secondary structure formation, we used all degenerate codons for both the randomized positions and the neighboring residues (Supplementary Fig. S4).

Expression levels of highly evolved clones only is limited by plasmid copy number

We had previously observed that a mutation in the origin of replication, resulting in a 2-fold increase in copy number, further enhanced expression levels of D03, a protein improved by evolution, whereas expression levels of the poorly folding rNTR1-wt remained unaffected.[11,22] Furthermore, both StEP library selections arrived at a plateau of expression levels at ~12,000 receptors per cell. We considered the possibility that the plasmid copy number was now limiting expression of the further evolved receptor mutants, which no longer have a limitation through folding and stability in the membrane. We therefore expressed the Slonomics® library in a vector with higher plasmid copy number (eLIC47; containing an engineered ColE1-derived origin,[23] abbreviated as L5). Expression levels were clearly further improved after five to six subsequent rounds of selection, with the MFI of L5 now reaching 6-fold that of D03 (Fig. 4a). In a parallel control experiment with the original plasmid pRGD03[11] (L1), the maximal MFI was only 3-fold that of D03, similar to the StEP libraries (Fig. 4b). This indeed suggests that, for the well-folding receptor mutant, the original copy number becomes limiting. The expression levels of individual variants reached more than 25,000 receptors per cell, a 50- to 60-fold increase compared to rNTR1-wt and even a 5-fold increase compared to D03 (Fig. 4c and d), the product of our first rNTR1 evolution.[11] High plasmid copy numbers thus only become useful with stable and well-folding GPCR variants, as the expression levels of D03 (with intermediate properties) is similar in pRGD03 and eLIC47, while expression of L5X is artificially limited by the lower copy number of pRGD03 (Fig. 5a).

We found that C7E02 is further stabilized by agonist binding, but the observed additional gain in stability is smaller than for unstable receptors such as D03 and rNTR1-wt (Table 2). Hence, we wished to screen for the most stable mutants in the presence of ligand directly. Evolved variants obtained from library L5, the Slonomics® library showing the highest functional expression after selection, were thus analyzed for their stability index in OG and *n*-heptyl-β-D-thioglucopyranoside (HTG), respectively, in the agonist-bound state (Fig. 6a). For that purpose, receptors were solubilized from the membrane and saturated with [^{3}H] neurotensin before incubation at elevated temperatures. The stability index, the ratio of remaining ligand binding activity after 20 min of incubation at the elevated temperature compared to incubation at 4 °C, thus represents the capacity of receptor to

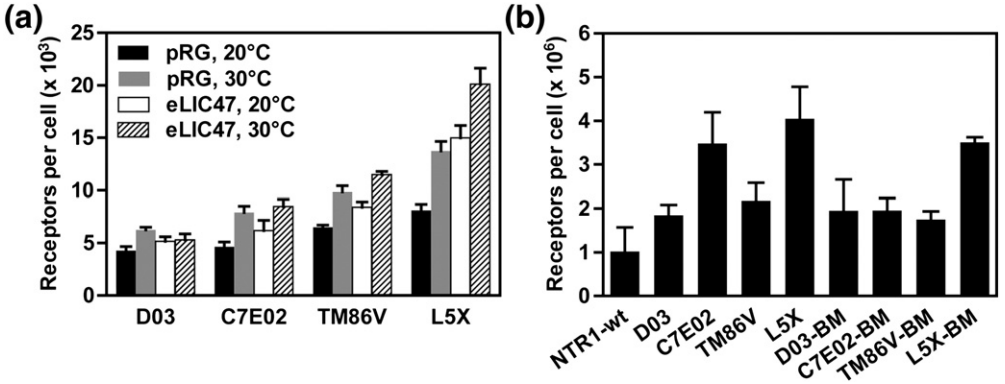

Fig. 5. Expression levels of evolved receptor variants (a) in comparison to D03 as a function of temperature and plasmid copy number in *E. coli* and (b) in *Sf9* cells. (a) D03 displays similar expression levels under all conditions, whereas C7E02, TM86V and L5X express better at 30 °C in both vectors. L5X expression is strongly increased in the high-copy-number eLIC47 vector that was used throughout the selection rounds. C7E02 and TM86V respond less to increased plasmid copy number of eLIC47. The average of three independent expression cultures, each measured in duplicate, is shown. (b) *Sf9* cells were infected at an MOI of 5 and harvested 62 h p.i. All evolved receptor variants are expressed at higher level compared to rNTR1-wt in *Sf9* cells [BM (=back-mutant) refers to restored DRY-motif (L167R$^{3.50}$)]. The average of three independent expressions, each measured in duplicate, is shown.

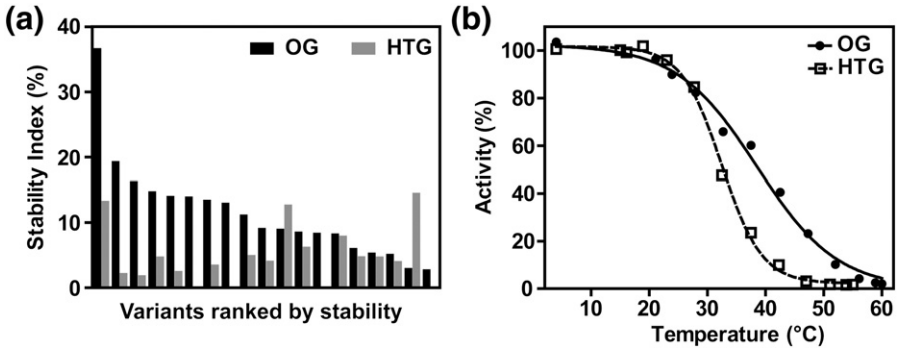

Fig. 6. Stability screening of Slonomics® library selections. (a) Stability screening in buffer SABoOG (0.8% OG as the sole detergent; black bars) and SABoHTG (1.5% HTG as the sole detergent; gray bars). Screening was performed in the agonist-bound state, for which the mutants were saturated with [^{3}H]neurotensin before incubation at elevated temperatures. The stability index is the ratio of remaining activity after 20 min of incubation at 45 °C compared to 4 °C. Only screened variants that retain ligand binding activity are shown. (b) Thermal denaturation profile of L5X, the most stable variant, in SABoOG (OG, filled circles) and SABoHTG (HTG, open squares) in the agonist-bound state. The apparent T_m is 38 °C in OG and 32 °C in HTG.

sustain ligand binding. About 40% of clones showed activity in OG and 30% even in HTG, and the most stable clone, L5X, behaved similarly in both detergents (Fig. 6b).

The apparent T_m of L5X in OG is 40 °C, another 10 °C gain compared to C7E02 and 33 °C in HTG (Fig. 6b and Supplementary Fig. S3d). In OG, L5X retains more than 75% activity after 72 h at 4 °C (Supplementary Fig. S5d), whereas HTG inactivates the receptor over time and is hence not suitable for further studies. L5X comprises 15 mutations, which only partially overlap with the C7E02 subset (Table 1). Agonist-bound L5X also shows high stability in milder detergents (Table 2 and Supplementary Fig. S3 and S5). In the ligand-free state, however, L5X is less stable than C7E02 in both DDM and DM, with a difference of 10° (Table 2 and Supplementary Fig. S2). These data reflect the screening and selection conditions that led to the identification of C7E02 or L5X, respectively, and suggest that L5X is preferentially stabilized in the agonist-bound state and that C7E02 is preferentially stabilized in the ligand-free state.

Structure-guided combination of mutations identified by evolution

We observed a strong correlation between higher functional expression levels and stability in detergents for the StEP and Slonomics® library selections. The effects from single shifts are small and not always significant,[13] and there may be a cooperative or synergistic effect of shifts selected together, making the effect much greater in the present libraries than with single randomized positions. We used the stability data in detergents for the single shifts[13] and for C7E02 (Table 1) to further investigate the contribution of the mutations to the stability increase in detergents and to generate a minimal C7E02-like variant. Here, we analyzed the combinatorial effects of the shifts A86L$^{1.54}$, I253A$^{5.54}$ and F358V$^{7.42}$ that are present in C7E02 and show the strongest effect on detergent stability when analyzed separately. The respective triple mutant, TM86V, was assembled and assayed for its detergent stability. In the ligand-free state, TM86V and C7E02 behave similarly, with C7E02 being slightly more stable in both DDM and DM (Table 2 and Supplementary Fig. S2). In the agonist-bound state, TM86V is superior to C7E02 in all detergents (Table 2 and Supplementary Fig. S3), and the effect is most pronounced in OG. Most important for practical applications such as functional assays and structure determination is that TM86V retains higher activity over time than C7E02 in all detergents in the agonist-bound state (Supplementary Fig. S5). It is thus similar to L5X in this respect (see above). TM86V is also expressed at a higher level than D03, but less than L5X (Fig. 5a).

Influence of the D03 mutation background

TM86V is a highly stable variant of D03, adding the three shift mutations A86L$^{1.54}$, I253A$^{5.54}$ and F358V$^{7.42}$ to D03. The three mutations partially overlap with NTS1-7m, an rNTR1-wt mutant identified by means of alanine-scanning mutagenesis.[18] We remade the NTS1-7m molecule in our laboratory and, in another molecule, introduced the three shifts A86L$^{1.54}$, I253A$^{5.54}$ and F358V$^{7.42}$ into rNTR1-wt (mutant wt-TTM) to test them under the same conditions. Both NTS1-7m and wt-TTM display detergent stability similar to each other in all detergents (Table 2), and both perform better than the unstable rNTR1-wt (Supplementary Fig. S2, S3 and S5). However, functional expression for both

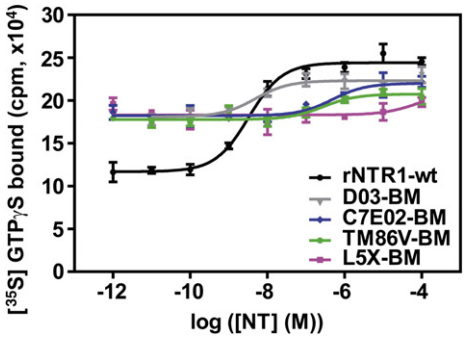

Fig. 7. Signaling activity of evolved receptor mutants. Agonist-stimulated nucleotide exchange at $G\alpha_{i1}$ of C7E02-BM, TM86V-BM and L5X-BM in comparison to rNTR1-wt and D03-BM [BM (=back-mutant) refers to restored DRY-motif ($L167R^{3.50}$)]. Triplicates of a representative experiment are shown (error bars represent standard deviation).

variants is only about 1.5-fold better than the low level of rNTR1-wt (Fig. S6). In contrast, with the evolved mutants C7E02, TM86V and L5X, which are all based on the D03 background, we reach detergent stabilities and expression levels that are greatly superior to NTS1-7m (Table 2 and Fig. 5a).

GPCR activation and signaling

The well-expressed and stable variants C7E02, L5X and TM86V were assayed for their signaling activity. D03 displays only low signaling activity in comparison to rNTR1-wt due to a mutation within the strongly conserved DRY-motif ($R167L^{3.50}$) that is crucial for activation of GPCRs.[24] A version of D03 with restored DRY-motif [D03-$L167R^{3.50}$, denoted in short as D03-BM (BM, *b*ack-*m*utant)] regains signaling activity,[11] and we have thus assayed C7E02, L5X and TM86V after reconstitution of the DRY-motif. For this purpose, we have used the *Spodoptera frugiperda* (*Sf9*) baculovirus system to coexpress our receptor variants with the G-protein $G\alpha_{i1}\beta_1\gamma_{10}$ and have used a nucleotide binding assay using [^{35}S]GTPγS to assess the stimulation of nucleotide exchange at $G\alpha_{i1}$ as a function of agonist binding to our receptor variants and suitable controls. Similar to expression in *E. coli*, C7E02, TM86V and L5X are expressed at a level similar to or higher than that of D03 in *Sf9* cells (Fig. 5b). Again, this underlines that functional expression is limited by physical features of the protein, and these features appear to be universal for prokaryotes and eukaryotes.

C7E02-$L167R^{3.50}$ (termed C7E02-BM) and TM86V-$L167R^{3.50}$ (termed TM86V-BM), both restored in their DRY-motif, induce exchange of GDP for GTPγS (Fig. 7). All mutants show about the same level of exchange as rNTR1-wt at high agonist concentrations but differ in their behavior at low agonist concentrations. Both C7E02-BM and TM86V-BM are characterized by a higher basal level than rNTR1-wt but still respond to agonist stimulation. The agonist affinities of the evolved receptor variants are very similar to that of D03 (Fig. 8a), excluding any possible influence of changes in agonist binding. The third very stable mutant, L5X-$L167R^{3.50}$ (L5X-BM), seems to be constitutively active, as it shows the same high nucleotide exchange activity independent of agonist concentration. Thus, all mutants are active in GDP/GTP exchange but differ in the degree by which the active state has been stabilized through selection even in the absence of bound agonist.

Discussion

To our knowledge, this is the first study reporting an increase of functional GPCR expression level in *E. coli* to more than 25,000 receptors per cell, starting from only 500 receptors per cell for rNTR1-wt, along

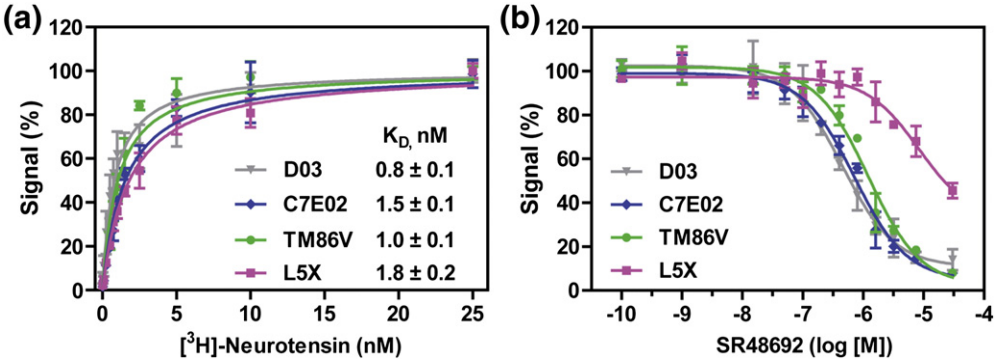

Fig. 8. Ligand binding affinities of the evolved receptor variants. (a) Agonist affinities of C7E02, TM86V and L5X in comparison to D03 was determined by equilibrium titration with [^{3}H]neurotensin using solubilized receptor immobilized via its C-terminus on magnetic beads. (b) Binding of antagonist SR 48692 to the receptor variants was measured by competition with 15 nM [^{3}H]neurotensin. (a and b) The average of two independent duplicate experiments is shown.

with unprecedented gains in detergent stability, such that receptors stable in OG were now obtained. We have also elucidated the structural reasons for this stability gain.

Previously observed apparent limits of functional GPCR expression after directed evolution must be attributed to limitations in exploring sequence space by random mutagenesis, as it does not allow all codon substitutions.[11,12] Our previous comprehensive position-specific mutational analysis of D03 showed that, indeed, only by fully exploring the sequence space, crucial substitutions for further optimization of functional expression and detergent stability could be identified.[13]

Maximization of both expression and stability required combination of some selected shift mutations with wild type in other positions, since some groups of selected shifts address the same problem, and only one of the shifts (but not all) should then be chosen. A binary library is the only way to find the optimal solution. Both approaches, the StEP recombination libraries and the binary (truly comprehensive) Slonomics® library, were successful in the identification of improved receptor variants. Moreover, the potential of the library could only be fully explored by removing measures originally taken to decrease toxicity of GPCR expression in *E. coli*, such as low expression temperatures and low plasmid copy number, as these measures were putting an artificial limit on functional expression (L5 *versus* L1).

During selection, pressure is applied on functional receptor expression, which is a result of the efficiency of correct protein folding, insertion into the lipid bilayer and stability within the lipid bilayer.[25] While host engineering has been successfully used to increase expression of some GPCRs in *E. coli*,[26] it does not address the intrinsic protein properties that limit downstream processes such as protein purification and functional assays in detergent solution. The high expression levels of our evolved receptor variants C7E02, TM86V and L5X are truly a result of the improved biophysical properties: C7E02, TM86V and L5X are also expressed at higher levels than D03 in different *E. coli* strains [e.g., BL21(DE3); data not shown] and *Sf9* insect cells (Fig. 5b). Previously, the higher expression of D03, compared to rNTR1-wt, was shown in *E. coli*, *Pichia pastoris* and human embryonic kidney 293 cells.[11] These results of the same mutants excelling in all expression systems emphasize that the effects are governed by the biophysical properties of the receptor.

In all library selections, functional receptor expression and detergent stability coevolved (Fig. 9), an effect that agrees well with our previous studies on different receptors, underlining the generality of the phenomenon.[11,12] Different from our selection technique, *in vitro* alanine scanning solely for detergent stability leads to uncoupling of receptor expression and stability, and coevolution is thus unlikely to be detected.[6,9] While in our approach, functional receptor expression and detergent stability are coupled, there are, besides mutations with overlapping effects, also individual mutations affecting functional expression only, which is mostly a measure of stability within the lipid bilayer, while others also influence stability in detergent micelles. The shift C332V$^{6.59}$, for example, is dominant after selection for functional expression but less relevant for detergent stability, as it even slightly reduces detergent stability of D03[13] and is found only in one of the three stable variants presented here. C332V$^{6.59}$ is located at the extracellular end of TM6, and it is the only free cysteine pointing toward the oxidizing milieu of the periplasmic space in *E. coli*. rNTR1 contains a disulfide bridge between C225 in extracellular loop 2 and C142$^{3.25}$ in TM3, and this particular shift mutation may mostly affect biosynthesis by preventing incorrect disulfide formation (see above) but not influence detergent stability per se. This hypothesis is supported by the 454 sequencing results obtained for positions C142$^{3.25}$ and C225 (for details, see Ref. 13).

However, not all shift mutations selected for high functional expression did significantly influence detergent stability, when studied individually.[13] Combined in M303, on the other hand, carrying all 33 shift mutations, this GPCR displays higher detergent stability than D03 (Supplementary Fig. S7b) yet is functionally expressed at a level similar to that of D03 (Supplementary Fig. S7a). Thus, individual mutations may also counteract the beneficial effect of others when combined. The selection from a combinatorial library, such as the StEP and Slonomics® libraries described here, can solve this problem. We observed cooperative effects of a subset of shift mutations with respect to detergent stability, and those positive effects seem to be dominant over any stability-decreasing effect of single mutations. Since the selection is for stability in the bilayer by means of functional expression level, both this property and stability in detergents coevolve.

TM86V is a minimal mutant of the selected C7E02, which still confers the desired phenotype. It combines the three shift mutations A86L$^{1.54}$, I253A$^{5.54}$ and F358V$^{7.42}$ with the most significant contribution to functional expression and detergent stability. For TM86V, the gain in detergent stability is additive, consistent with the fact that, according to an rNTR1 homology model, these shift mutations are not in a distance where they could interact with each other (Fig. 10). Moreover, these three shift mutations have a positive effect on detergent stability on both the rNTR1-wt background (wt-TTM) and the already evolved D03 background (TM86V; Table 2 and Supplementary Fig. S2, S3 and S5), emphasizing that positions with crucial relevance for improving the biophysical properties of rNTR1 were found,

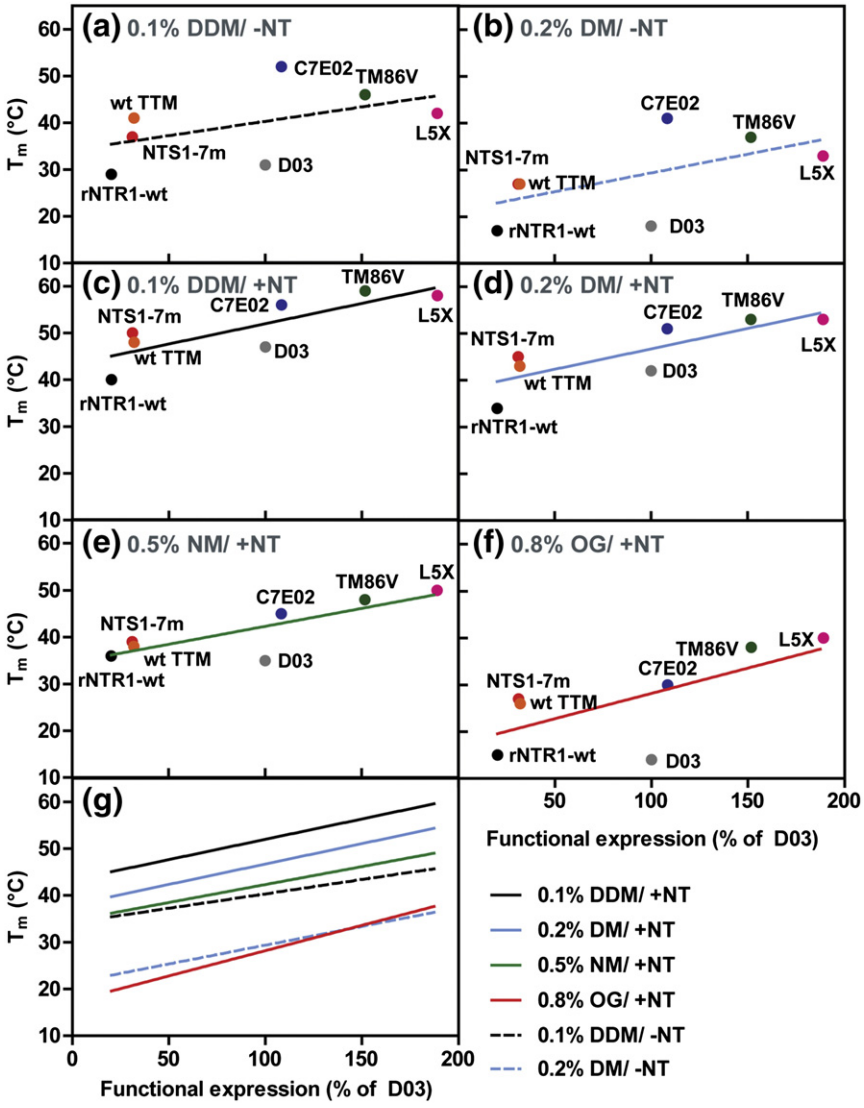

Fig. 9. Correlation between functional expression and detergent stability. The functional expression levels relative to D03 (expression in vector pRGD03, 20 h at 20 °C) are plotted against detergent stability.(a) Ligand-free state in DDM, (b) ligand-free state in DM, (c) agonist-bound state in DDM, (d) agonist-bound state in DM, (e) agonist-bound state in NM, and (f) agonist-bound state in OG. The linear regressions [black broken lines in (a)–(f) are replotted in (g)]. The correlation between high functional expression and detergent stability is highest for harsher detergent conditions, that is, DM in the absence of agonist (b) and OG in the presence of agonist (f).

independent of the receptor variant (rNTR1-wt or D03). It should be noted, however, that the maximal stabilizing effects and the maximal expression levels can only be obtained in the D03 background, which is already a product of directed evolution (Table 2, Fig. 5 and Supplementary Fig. S6).

As discussed in Schlinkmann *et al.*,[13] I253A$^{5.54}$, pointing toward the helical core, might restrict conformational flexibility of the receptor and increase compactness of the helical core, thus leading to increased detergent stability, while A86L$^{1.54}$ and F358V$^{7.42}$ might optimize helix packing, thus decreasing the sensitivity to detergent denaturation.

The selected variants TM86V and C7E02 retain agonist-stimulated signaling activity, that is, activation of heterotrimeric G-proteins, which is intriguing considering that this particular characteristic was never under direct selection pressure. The determination of the transition point for rNTR1-wt is very robust (log [EC_{50}] = −8.5 ± 0.1) but more uncertain for D03 and the evolved receptor variants as a result of the small changes in total signal. The increased level of basal activation can most probably be attributed to partial stabilization of the receptor variant in the activated state as a consequence of the applied selection pressure in the presence of agonist. While all evolved variants are characterized by high

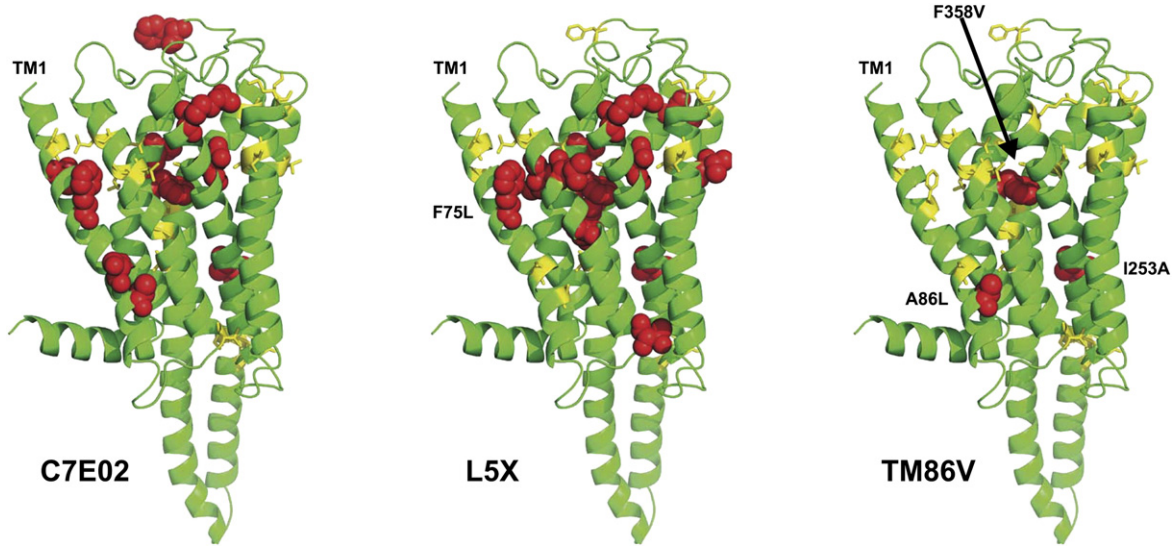

Fig. 10. Homology model of C7E02, L5X and TM86V. The 33 StEP-shuffled positions are highlighted in yellow. The positions of mutations in C7E02, L5X and TM86V in comparison to D03 are highlighted in red spheres (the D03 amino acid is given). For C7E02 and L5X, some mutations are in a distance where they could possibly interact. Generation of the homology model is described in detail in Ref. 13.

basal activity, stabilization of the agonist-bound state is strongest for L5X, which does not respond to agonist stimulation. This hypothesis of selected stabilization of the agonist-bound state is strongly supported by the high detergent stability of L5X in the agonist-bound state and, particularly, by the strongly decreased affinity of L5X to bind the small-molecule antagonist SR 48692[27] in comparison to D03 as well as to TM86V and C7E02 (Fig. 8b).

Nevertheless, the high basal activity of the receptor variants observed could in principle also result from higher functional expression of the above variants compared to rNTR1-wt. However, higher basal activity is only observed after reconstitution of the DRY-motif (L167R$^{3.50}$ back-mutation), suggesting that this phenomenon is signaling dependent and a true property of the evolved receptors. Additionally, although the G-protein coexpression levels between different receptor variants were carefully adjusted using quantitative Western blots, the quantitative comparison of receptor variants in this assay remains difficult and is of limited accuracy (cf. Ref. 28, chapter 12). Here, we have shown that the evolved receptor mutants are signaling-active, but the detailed characterization of G-protein binding and activation will be the focus of a separate study.

All three variants (TM86V, C7E02 and L5X) contain F358V$^{7.42}$, a position in TM7 that, when mutated to alanine, is known to confer constitutive activity.[29] The valine substitution in our variants retains agonist-dependent stimulation of signaling in C7E02 and TM86V, albeit with an increased basal activity, and may thus be an intermediate conformation. The fact that L5X is indeed constitutively active must then be due to further effects, such as a strong rigidification as a result of small additive effects of its 15 shift mutations.

With C7E02, TM86V and L5X, we have a unique set of evolved receptor variants with improved expression levels and stability in detergents. Despite their mutational load, all three variants are still highly identical with rNTR1-wt (TM86V is 97% identical; C702, 95%; L5X, 94%). Their improved biophysical properties will facilitate structural studies, and their differences in signaling activity will help in functional investigation of rNTR1.

In summary, we show that, by fully exploring the enormous sequence space of a GPCR by a directed evolution approach, we can arrive at molecules that are functional in agonist binding and signaling and are stable in short-chain detergents, and we can reach the expression level of abundant bacterial membrane proteins. In this proof-of-principle experiment, we proceeded in three steps. After initial random mutagenesis, an improved variant was evolved (D03),[11] with which a comprehensive evaluation of every codon at every position became possible.[13] By now screening a comprehensive *binary* library of all "shifted" amino acids with their D03 counterparts, we obtained variants with 50-fold improved expression levels and with stability in detergents as short as octylglucoside. The insight into the parts of the GPCR critical for stability both in the bilayer membrane and in detergents that has been reached in the present study may allow to greatly shortcut this approach for other GPCRs by already introducing a number of these changes identified here.

Materials and Methods

StEP library design and generation

The D03 gene and either the synthetic M30 or the M303 gene were used as input for *in vitro* DNA shuffling using the StEP (see Supplementary Fig. S1 for illustration) using the amplification primers NTR1longfw (CGCGCAGACTGGATCTAACAACAACAACAATAAC) and NTR1longrev (CAGAACCGCCACCAGAACCGCCACCG). We mixed 10 ng of each template DNA per 50 µl PCR reaction using $Vent_R$® DNA Polymerase (NEB) and 30 pmol of each flanking primer, introducing a restriction site. Shuffling was performed for 125 cycles on a Biometra T3 cycler with 30 s of denaturation (94 °C) and 6 s of annealing/elongation at 50 °C and 2 min of initial denaturation. Twelve reactions were run in parallel. The PCR product was treated with DpnI (Fermentas) for digestion of the input DNA that was obtained from propagation of the template plasmid in *E. coli*. The StEP product was then purified from a preparative 1.5% agarose gel. The purified DNA was digested with BamHI (NEB) and Cfr9I (Fermentas), and 3 µg of purified DNA was ligated into 5 µg of vector pRGD03[11] (insert in 3-fold molar excess) overnight at 16 °C. Ligation products were purified using Qiagen MinElute PCR purification columns, eluted in a total volume of 20 µl of 2 mM Tris–Cl (pH 8.5) and used for electroporation of 500-µl electrocompetent *E. coli* DH5α cells. Cells were recovered in 5 ml SOC medium for 1 h at 37 °C and further cultivated in 500 ml 2YT medium supplemented with 1% glucose and 100 µg/ml ampicillin for 12–16 h at 28 °C. Dilution series were plated on 2YT–agar plates (1.5% agar, 1% glucose and 100 µg/ml ampicillin) to determine the library size. Typically, the library size was between 5×10^7 and 3×10^8. Aliquots of $>10^9$ cells were supplemented with 20% glycerol, snap-frozen in liquid N_2 and stored at −80 °C until further use.

Slonomics® library design and generation

The design of the library is schematically shown in Supplementary Fig. S4. The 33 randomized positions contain all codons specifying both the D03-specific residue and the respective shift residue. All degenerate codons were equally represented in order to exclude any bias due to codon usage, tRNA levels or mRNA secondary structure formation. For the same reason, the positions flanking the randomized positions were also represented equally with all codons for the respective amino acid except at three positions (L74, L343 and L357) where a single leucine codon (CTC) was omitted to avoid the generation of specific restriction enzyme motifs. Thus, on the amino acid level, the library is binary and equimolar, and on the nucleotide level, it is agnostic. On the amino acid level, the library diversity is $2^{33}=8.5\times10^9$. The library was generated by the Slonomics® technology[16,17] and shipped as a linear DNA fragment. The library DNA was then amplified using the amplification primers SLK_fw2 (CCAGTCTGGATCCACCTCGGAATCCGACACGGCAGGGCCC) and SLK_rev1 (GAAGTACAGGTTCTCCCGGGTAGCGCAGGTGGAAAAGGCA). Cloning and transformation was performed as for the StEP libraries. Transformation efficiencies and thus library diversity were 3×10^8 for L1 and 1.3×10^8 for L5.

Library expression and selection

Libraries were expressed in 60 ml 2YT medium with 0.2% glucose and 100 µg/ml ampicillin. Cultures were inoculated to $OD_{600}=0.05$ and grown at 37 °C to $OD_{600}=0.5$, at which time protein expression was induced with 250 µM IPTG and continued for 20 h at 20 °C or 30 °C, respectively. For all libraries, the first two rounds of selection were performed with an expression temperature of 20 °C, after which the expression temperature was increased to 30 °C. An aliquot of cells was washed in ice-cold TKCl buffer [50 mM Tris–HCl (pH 7.4) and 150 mM KCl] and saturated with 20 nM BODIPY-neurotensin (8–13) for 1–2 h at 4 °C. Nonspecific binding was determined in the presence of 10 µM neurotensin (8–13). Cells were washed twice in TKCl buffer and resuspended in 1 ml TKCl buffer. Selections were performed on a BD FACS Aria I (Flow Cytometry Laboratory, UZH/ETHZ), and 100,000 cells of the top 1% expressing cells were isolated in the yield mode (selection of naïve libraries) or purity mode (all further selections). Selected cells were directly sorted into 2 ml 2YT medium (1% glucose and 100 µg/ml ampicillin), recovered for 1–2 h at 37 °C, diluted into 30 ml 2YT (1% glucose and 100 µg/ml ampicillin) and grown for 12–16 h at 28 °C. Aliquots of $>10^8$ cells were supplemented with 20% glycerol, snap-frozen in liquid N_2 and stored at −80 °C until further use.

Whole-cell radioligand binding assays

Radioligand binding assays (RLBAs) were used to quantify receptor expression levels. Expression in *E. coli* was performed essentially as described for library expression (see above), whereas in *S. frugiperda* (*Sf9*) 10^7 cells were seeded as monolayer in 10-cm cell culture dishes, infected at an MOI (*m*ultiplicity *o*f *i*nfection) of 5 with the respective virus and harvested 62 h p.i. (*p*ost-*i*nfection). To allow for agonist binding, we resuspended 10^7 *E. coli* cells or 10^5 *Sf9* cells in 200 µl TEBB buffer [50 mM Tris–HCl (pH 7.4), 1 mM ethylenediaminetetraacetic acid (EDTA), 0.1% (w/v) BSA (*b*ovine *s*erum *a*lbumin) and 40 µg/ml bacitracin] containing 15 nM [^{3}H]neurotensin (PerkinElmer) and incubated for 2 h at 4 °C. Nonspecific binding was determined in the presence of 5 µM unlabeled agonist. Cells were applied to glass fiber filters (Millipore), separated from free ligand using a 96-well vacuum manifold (Millipore) and washed four times with 200 µl TEBB buffer. Filters were dried for 1 h at 60 °C and allowed to dissolve in 200 µl OptiPhase SuperMix (PerkinElmer) for 6–14 h. Filter-bound radioactivity was measured by liquid scintillation counting (Microbeta 1450 Plus liquid scintillation counter; Wallac).

Analysis of detergent stability

Stability measurements of evolved receptor variants in the ligand-free state were essentially performed as described previously.[12] All stability assay buffers contained 50 mM Hepes (pH 7.4), 100 mM NaCl, 1 mM EDTA and Complete Protease Inhibitor (Roche). Buffer

SAB additionally contained 30% glycerol and 0.1% (w/v) DDM (Anatrace), 0.5% (w/v) Chaps (Anatrace) and 0.1% (w/v) CHS (Sigma-Aldrich); buffer SABoDDM contained 0.1% (w/v) DDM; buffer SABoDM contained 0.2% (w/v) DM (Anatrace); buffer SABoNM contained 0.5% (w/v) NM (Anatrace); buffer SABoOG contained 0.8% (w/v) OG (Anatrace) and buffer SABoHTG contained 1.5% HTG (Anatrace). Detergent and glycerol concentrations for ligand binding buffers were changed accordingly. For all measurements, receptors were solubilized in DM, and detergent was exchanged after immobilization (Dynabeads® MyOne™ Streptavidin T1; Invitrogen). For detergent exchange, beads were captured using a magnetic tube holder, and beads were washed two times with 150 μl of desired assay buffer for 5 min each and resuspended in a final volume of 150 μl assay buffer. For stability measurements in the agonist-bound state, receptors were solubilized in DM and saturated with 120 nM [^{3}H]neurotensin (PerkinElmer) in a volume of 150 μl for 90 min, before detergent exchange. Data were analyzed by nonlinear regression using GraphPad Prism 5.

Affinity measurements

Receptors were solubilized and immobilized in DM as described in Ref. 12. Aliquots of the receptors immobilized on magnetic beads were incubated with increasing concentrations of the agonist [^{3}H]neurotensin in a volume of 200 μl for 2 h at 4 °C in assay buffer LBB-DM [50 mM Tris–HCl (pH 7.4), 0.2% DM, 1 mM EDTA, 0.1% (w/v) BSA and protease inhibitor (Complete Protease Inhibitor Cocktail; Roche)]. Unbound agonist was removed by capturing the beads using a magnetic tube holder and washing of the beads with 200 μl of buffer LBB-DM. Receptor-bound agonist was quantitated by liquid scintillation counting. Data were analyzed by nonlinear regression using GraphPad Prism 5. Binding of the antagonist SR 48692 was determined accordingly by titration of SR 48692 in the presence of 15 nM [^{3}H]neurotensin.

[^{35}S]GTPγS binding assay

Receptors and the G-protein ($\alpha_{i1}\beta_1\gamma_{10}$) were expressed in *S. frugiperda* (*Sf9*) cells by co-infection with two baculoviruses, one encoding the receptor and the other encoding the whole G-protein complex. Baculoviruses were generated essentially as described for the MultiBac system.[30,31] Receptors were preceded by an N-terminal melittin signal sequence, a FLAG tag, a His_{10} tag and a TEV cleavage site, whereas the C-terminus was unmodified. The $G\alpha_{i1}$ subunit was internally His_6 tagged at position 121,[32] γ_{10} was N-terminally HA tagged and β_1 was untagged.

Sf9 cells at a density of 1×10^6 cells/ml were co-infected with receptor virus and G-protein virus at a MOI of 2 and 1, respectively. At 72 h p.i., cells were harvested by centrifugation (10 min, 500*g*, 4 °C) and washed with phosphate-buffered saline twice. Cells were resuspended in lysis buffer [50 mM Tris–HCl (pH 8.0), 1 mM EDTA and protease inhibitor (Complete Protease Inhibitor Cocktail; Roche)] and were lysed by sonication. The lysate was centrifuged (10 min, 500*g*, 4 °C), and the resulting supernatant was centrifuged again (30 min, 20,000*g*, 4 °C). The membrane pellet was washed once with lysis buffer, and the membranes were finally resuspended in lysis buffer containing 20% sucrose and flash-frozen. Protein concentration was determined by the Quant-iT™ Protein Assay Kit (Life Technologies), and expression was controlled by quantitative IR Western blot analysis using the Odyssey® system (LI-COR).

Stimulation of [^{35}S]GTPγS (1250 Ci/mmol; PerkinElmer) binding was performed with 20 μg membrane protein in 100 μl binding buffer [50 mM Tris–HCl (pH 7.4), 5 mM $MgCl_2$, 50 mM NaCl, 1 mM EDTA, 0.1% (w/v) BSA, 0.1 mM DTT, 1 μM 1,10-phenanthroline and 1 μM GDP] containing various neurotensin concentrations (2 pM–200 μM). After preincubation (15 min at room temperature), 100 μl binding buffer with 2 nM [^{35}S]GTPγS (final concentration, 1 nM) was added, and the mixture was further incubated (45 min at room temperature). The reaction was stopped by filtration through 96-well MultiScreen glass fiber filter plates (Millipore) and washed five times with 200 μl washing buffer [50 mM Tris–HCl (pH 7.4), 5 mM $MgCl_2$, 50 mM NaCl and 1 mM EDTA]. Filter-bound radioactivity was determined by liquid scintillation counting.

Acknowledgements

We would like to thank Stefan Heiderich for excellent technical assistance during Slonomics® library synthesis and Annemarie Honegger for preparation of the rNTR1 homology model (Fig. 10). We are thankful to Anette Schütz and Malgorzata Kisielow (Flow Cytometry Laboratory, ETHZ/UZH) for expert technical support during FACS selections. This work was supported by a grant from the NCCR Structural Biology (Swiss National Science Foundation) to A.P.

Author Contributions. K.M.S. designed and generated the StEP libraries. R.S. planned and supervised the Slonomics® library synthesis project. K.M.S. performed FACS selections and analysis of the StEP libraries and Slonomics® libraries. K.M.S. performed expression analysis in *E. coli*, detergent stability and affinity measurements. M.H. and A.R. designed and performed signaling and expression analysis experiments in *Sf9* cells. M.K. helped in the optimization of signaling assay conditions. A.P. planned and supervised the project. K.M.S. and A.P. wrote the manuscript.

Supplementary Data

Supplementary data to this article can be found online at http://dx.doi.org/10.1016/j.jmb.2012.05.039

References

1. Lagerström, M. C. & Schiöth, H. B. (2008). Structural diversity of G protein-coupled receptors and significance for drug discovery. *Nat. Rev., Drug Discov.* **7**, 339–357.
2. Overington, J. P., Al-Lazikani, B. & Hopkins, A. L. (2006). How many drug targets are there? *Nat. Rev., Drug Discov.* **5**, 993–996.
3. Jaakola, V. P., Griffith, M. T., Hanson, M. A., Cherezov, V., Chien, E. Y., Lane, J. R. *et al.* (2008). The 2.6 Ångström crystal structure of a human A_{2A} adenosine receptor bound to an antagonist. *Science*, **322**, 1211–1217.
4. Cherezov, V., Rosenbaum, D. M., Hanson, M. A., Rasmussen, S. G., Thian, F. S., Kobilka, T. S. *et al.* (2007). High-resolution crystal structure of an engineered human β_2-adrenergic G protein-coupled receptor. *Science*, **318**, 1258–1265.
5. Rosenbaum, D. M., Cherezov, V., Hanson, M. A., Rasmussen, S. G., Thian, F. S., Kobilka, T. S. *et al.* (2007). GPCR engineering yields high-resolution structural insights into β_2-adrenergic receptor function. *Science*, **318**, 1266–1273.
6. Warne, T., Serrano-Vega, M. J., Baker, J. G., Moukhametzianov, R., Edwards, P. C., Henderson, R. *et al.* (2008). Structure of a β_1-adrenergic G-protein-coupled receptor. *Nature*, **454**, 486–491.
7. Wu, B., Chien, E. Y., Mol, C. D., Fenalti, G., Liu, W., Katritch, V. *et al.* (2010). Structures of the CXCR4 chemokine GPCR with small-molecule and cyclic peptide antagonists. *Science*, **330**, 1066–1071.
8. Chien, E. Y., Liu, W., Zhao, Q., Katritch, V., Han, G. W., Hanson, M. A. *et al.* (2010). Structure of the human dopamine D3 receptor in complex with a D2/D3 selective antagonist. *Science*, **330**, 1091–1095.
9. Serrano-Vega, M. J., Magnani, F., Shibata, Y. & Tate, C. G. (2008). Conformational thermostabilization of the β_1-adrenergic receptor in a detergent-resistant form. *Proc. Natl Acad. Sci. USA*, **105**, 877–882.
10. Rasmussen, S. G., DeVree, B. T., Zou, Y., Kruse, A. C., Chung, K. Y., Kobilka, T. S. *et al.* (2011). Crystal structure of the β_2 adrenergic receptor–Gs protein complex. *Nature*, **477**, 549–555.
11. Sarkar, C. A., Dodevski, I., Kenig, M., Dudli, S., Mohr, A., Hermans, E. & Plückthun, A. (2008). Directed evolution of a G protein-coupled receptor for expression, stability, and binding selectivity. *Proc. Natl Acad. Sci. USA*, **105**, 14808–14813.
12. Dodevski, I. & Plückthun, A. (2011). Evolution of three human GPCRs for higher expression and stability. *J. Mol. Biol.* **408**, 599–615.
13. Schlinkmann, K. M., Honegger, A., Tureci, E., Robison, K. E., Lipovsek, D. & Plückthun, A. (2012). Critical features for biosynthesis, stability and functionality of a G protein-coupled receptor uncovered by all-*versus*-all mutations. *Proc. Natl Acad. Sci. USA*, **109**, 9810–9815.
14. Zhao, H. & Zha, W. (2006). *In vitro* "sexual" evolution through the PCR-based staggered extension process (StEP). *Nat. Protoc.* **1**, 1865–1871.
15. Aguinaldo, A. M. & Arnold, F. (2002). Staggered extension process (StEP) *in vitro* recombination. *Methods Mol. Biol.* **192**, 235–239.
16. Van den Brulle, J., Fischer, M., Langmann, T., Horn, G., Waldmann, T., Arnold, S. *et al.* (2008). A novel solid phase technology for high-throughput gene synthesis. *BioTechniques*, **45**, 340–343.
17. Zhai, W., Glanville, J., Fuhrmann, M., Mei, L., Ni, I., Sundar, P. D. *et al.* (2011). Synthetic antibodies designed on natural sequence landscapes. *J. Mol. Biol.* **412**, 55–71.
18. Shibata, Y., White, J. F., Serrano-Vega, M. J., Magnani, F., Aloia, A. L., Grisshammer, R. & Tate, C. G. (2009). Thermostabilization of the neurotensin receptor NTS1. *J. Mol. Biol.* **390**, 262–277.
19. Ballesteros, J. A. & Weinstein, H. (1992). Analysis and refinement of criteria for predicting the structure and relative orientations of transmembranal helical domains. *Biophys. J.* **62**, 107–109.
20. Ostermeier, C. & Michel, H. (1997). Crystallization of membrane proteins. *Curr. Opin. Struct. Biol.* **7**, 697–701.
21. Park, J. H., Scheerer, P., Hofmann, K. P., Choe, H. W. & Ernst, O. P. (2008). Crystal structure of the ligand-free G-protein-coupled receptor opsin. *Nature*, **454**, 183–187.
22. Tucker, J. & Grisshammer, R. (1996). Purification of a rat neurotensin receptor expressed in *Escherichia coli*. *Biochem. J.* **317**, 891–899.
23. Bayer, K., Grabherr, R., Nilsson, E. & Striedner, G. (2007). Expression vectors with modified ColE1 origin of replication for control of plasmid copy number European Patent EP 1 326 989 B1.
24. Rovati, G. E., Capra, V. & Neubig, R. R. (2007). The highly conserved DRY motif of class A G protein-coupled receptors: beyond the ground state. *Mol. Pharmacol.* **71**, 959–964.
25. Jungnickel, B., Rapoport, T. A. & Hartmann, E. (1994). Protein translocation: common themes from bacteria to man. *FEBS Lett.* **346**, 73–77.
26. Skretas, G. & Georgiou, G. (2010). Simple genetic selection protocol for isolation of overexpressed genes that enhance accumulation of membrane-integrated human G protein-coupled receptors in *Escherichia coli*. *Appl. Environ. Microbiol.* **76**, 5852–5859.
27. Labbe-Jullie, C., Botto, J. M., Mas, M. V., Chabry, J., Mazella, J., Vincent, J. P. *et al.* (1995). [^{3}H]SR 48692, the first nonpeptide neurotensin antagonist radioligand: characterization of binding properties and evidence for distinct agonist and antagonist binding domains on the rat neurotensin receptor. *Mol. Pharmacol.* **47**, 1050–1056.
28. Manning, D. R. (1999). *G proteins: techniques of analysis.* CRC Press.
29. Barroso, S., Richard, F., Nicolas-Etheve, D., Kitabgi, P. & Labbe-Jullie, C. (2002). Constitutive activation of the neurotensin receptor 1 by mutation of Phe(358) in helix seven. *Br. J. Pharmacol.* **135**, 997–1002.
30. Fitzgerald, D. J., Berger, P., Schaffitzel, C., Yamada, K., Richmond, T. J. & Berger, I. (2006). Protein complex expression by using multigene baculoviral vectors. *Nat. Methods*, **3**, 1021–1032.
31. Bieniossek, C., Imasaki, T., Takagi, Y. & Berger, I. (2012). MultiBac: expanding the research toolbox for multiprotein complexes. *Trends Biochem. Sci.* **37**, 49–57.
32. Kozasa, T. (2004). Purification of G protein subunits from Sf9 insect cells using hexahistidine-tagged a and bg subunits. *Methods Mol. Biol.* **237**, 21–38.